Communication
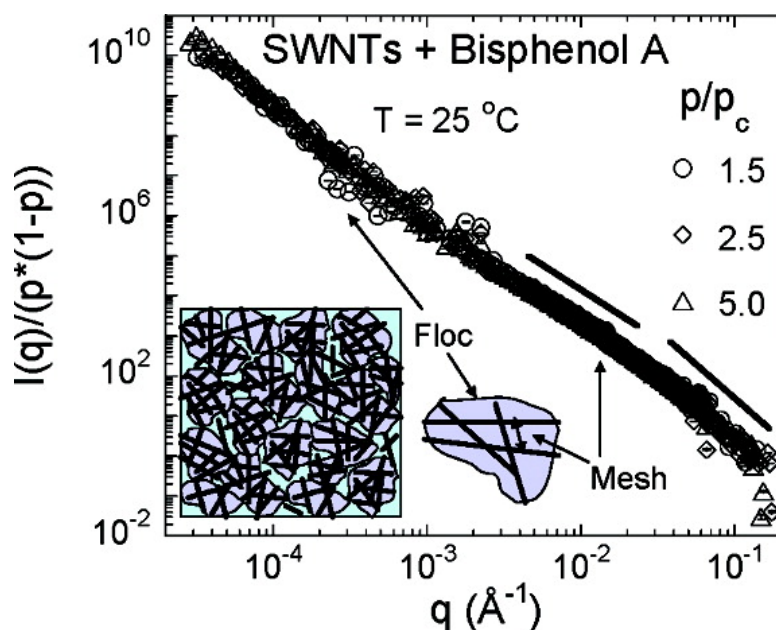
Hierarchical Structure of Carbon Nanotube Networks

Tirtha Chatterjee, Andrew Jackson, and Ramanan Krishnamoorti

More About This Article

Additional resources and features associated with this article are available within the HTML version:

- Supporting Information
- Links to the 1 articles that cite this article, as of the time of this article download
- Access to high resolution figures
- Links to articles and content related to this article
- Copyright permission to reproduce figures and/or text from this article

View the Full Text HTML

Hierarchical Structure of Carbon Nanotube Networks

Tirtha Chatterjee,[†] Andrew Jackson,[‡] and Ramanan Krishnamoorti*,[†]

Department of Chemical and Biomolecular Engineering, University of Houston, Houston, Texas 77204-4004, NIST Center for Neutron Research, National Institute of Standards and Technology, Gaithersburg, Maryland 20899-6102, and Department of Materials Science and Engineering, University of Maryland, College Park, Maryland 20742-2115

Received February 27, 2008; E-mail: ramanan@uh.edu

Dispersing nanoparticles in polymeric and nonpolymeric matrices has attracted significant scientific and technological interest. Semidilute dispersions of spherical silica nanoparticles, spherical and fractal carbon black, rod-like nanotubes, and disk-like silicates in solvents and low molecular weight polymers have demonstrated remarkable simplicity in their rheological properties.[1,2] Specifically, dispersions with particle concentrations in excess of percolation ($p \gg p_c$, where p is the volume fraction of the nanoparticles and p_c is the value at percolation) demonstrate time−temperature-composition superposition in their linear viscoelastic response that is dominated by the gel-like character arising from the network superstructure of the nanoparticles.[1−3] The modulus of the network of nanoparticles scales as $(p - p_c)^\delta$, with δ ranging between 2.5 and 4.5 for most cases, and is argued to be caused by the formation of fractal superstructures between weakly attractive contacts without significant dependence on the chemical and topological identity of the primary nanoparticles underlying the superstructure.[1−3] The most significant issue that needs to be resolved is the role of the micronsized flocs, ubiquitous in such dispersions, and that of the detailed internal structure within such flocs, which can be characterized by interactions between structural elements separated by distances of the order of the mesh-size of the networks. In this communication, we present detailed structural data suggesting that the interactions between aggregated clusters (or flocs) are responsible for such concentration-independent behavior.

Single-walled carbon nanotubes dispersed in two different epoxy matrices (bisphenol A (BA) and bisphenol F (BF)) as well as in a low molecular weight polymer matrix (polyethyleneoxide (PEO), $M_w = 8000$ Da) were selected as the model systems. The viscosities (η^0) of these systems are comparable and range from 0.7 to 2.2 PaS at the measurement conditions. A wide concentration window ($2 \le p/p_c \le 15$), with the upper limit being set by the large Onsager potential of the anisotropic particles leading to nematic structures at higher concentrations,[1,4] is examined. These systems thus represent a semidilute dispersion of nanoparticles, a range of significant practical importance as well as largely unexplored systematically in terms of structure. Detailed studies on the dispersion state and linear rheology of some of these systems have been published elsewhere.[1,5]

Small and ultrasmall angle neutron scattering (SANS and USANS[6]) are ideal techniques to probe the hierarchical structure expected from such a network. These measurements were performed at NIST (Gaithersburg, MD), over a broad range of scattering vector q ($=4\pi/\lambda \sin(\theta/2)$, where λ and θ are the wavelength and scattering angle) values. The q dependence of the scattered intensity, $I(q)$, was roughly independent of nanotube loading over the entire q range (3×10^{-5} Å^{-1} < q < 0.1 Å^{-1}). The scattered intensity, when
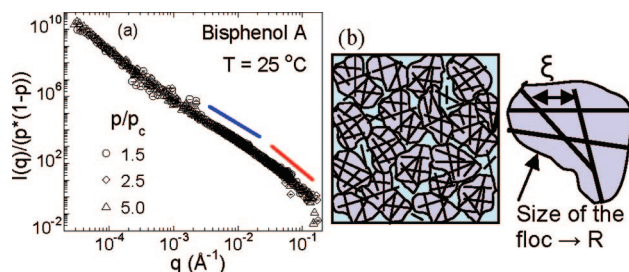
Figure 1. (a) Concentration effect corrected scattering data lead to a master curve indicating a hierarchical network structure over a wide length scale range. (b) A schematic of the hierarchical network structure showing different length scales; we note that the mesh size and floc sizes could be quite polydisperse.

scaled by $p \times (1 - p)$ (expected for disordered systems), forms a mastercurve as shown in Figure 1a.

A schematic of the hypothesized nanotube network is shown in Figure 1b. On a macroscopic scale, a matrix spanning network is formed which consists of numbers of aggregated clusters or flocs. The associated length scale is the average density correlation length between two clusters corresponding to the average cluster/floc size (R). Inside the floc, individual or small bundles of tubes (depending on the dispersion state) overlap each other, and the average distance between two adjacent contacts is the network mesh size (ζ). We note that, at the concentrations studied, the fraction of individualized nanotubes is small and thus the characteristic scattering from individual nanotubes is absent as has been reported previously for such nanotube networks.[7]

Scattering from hierarchical fractal structures can be described by a unified equation[8] with multiple structural levels:

$$I(q) = \sum_{i=1,2} G_i \exp\left(-\frac{q^2 R_{g,i}^2}{3}\right) + B_i\left\{\left[erf\left(\frac{qR_{g,i}}{\sqrt{6}}\right)\right]^3 \Big/ q\right\}^{y_i} \quad (1)$$

where the scattering from each structural level is expressed as the combination of a q-independent Guinier behavior and structurally limited power law scattering, considering both as independent scatterings sources. G_i and B_i are Guinier and power law prefactors, respectively. The length scales and the fractal dimension associated with each structural level are given by $R_{g,i}$ and y_i, respectively. On the basis of the observed scattering data (Figures 1a and 2a), a two-level ($i = 1, 2$) unified equation is used and the fitting shows good agreement with the experimental data (Figure 2a). The extracted length scales are identified as the floc ($R_{g,1} = R$) and the mesh size ($R_{g,2} = \zeta$) of the network and the corresponding power law exponents are the overall mass fractal dimension ($y_1 = d_f$) and the mesh fractal dimension ($y_2 = d_{mesh}$) of the structure. Some relevant structural parameters obtained from the fitting are summarized in Table 1.

† University of Houston.
‡ National Institute for Standard and Technology and University of Maryland.
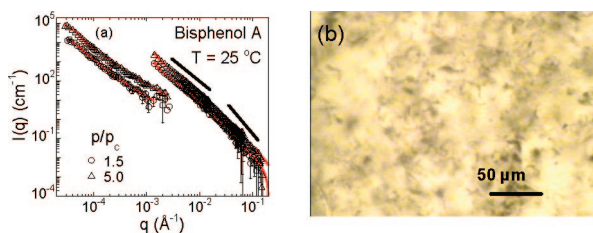
Figure 2. (a) A representative fitting[9] of the smeared unified model to the scattering data. The shifts in intensity between the SANS and USANS data are due to differences in instrument resolution functions. (b) Optical microscope image of a representative dispersion ($p/p_c = 4.0$; PEO) verifies the presence of micron-sized flocs (see Table 1).

**Table 1.** Unified Model Fit Results of the Scattering Data

p/p_c	fractal dimension (d_f)	floc size (μm)
Bisphenol F		
1.2	2.9 ± 0.1	4.3 ± 0.2
2.0	2.9 ± 0.1	4.4 ± 0.2
4.0	2.9 ± 0.1	3.6 ± 0.1
Bisphenol A		
1.5	3.0 ± 0.1	4.1 ± 0.2
2.5	2.9 ± 0.1	4.4 ± 0.3
5.0	2.9 ± 0.1	4.9 ± 0.1
PEO		
4	2.4 ± 0.1	3.9 ± 0.4
6	2.3 ± 0.3	3.2 ± 0.2
7	2.3 ± 0.2	3.5 ± 0.2
8	2.2 ± 0.3	3.8 ± 0.4
10	2.3 ± 0.1	3.3 ± 0.3
15	2.2 ± 0.2	3.6 ± 0.2

The average mass fractal dimension (d_f) of the SWNT's network is found to be a function of the dispersion state. The PEO dispersions show a lower p_c (0.09 vol %) and demonstrate a lower d_f value ~2.3 ± 0.2. In the epoxy resin matrices, the d_f values are ~3.0, consistent with the higher values of p_c (0.2−0.25 vol %).

While the higher molecular weight PEO is expected to have higher entropic barriers to dispersion compared to epoxy matrices, the absence of compatibilizers to aid tube dispersion in the epoxy results in denser particle aggregates leading to higher d_f values. The mesh fractal dimension (d_{mesh}) is higher than d_f for all the samples denoting a crowded structure at that length scale (Supporting Information). On the other hand, the average floc size is found to be roughly independent of the dispersion state, particle concentration, and the dispersing medium. The presence of such micron scale flocs is also confirmed by the optical microscope image (Figure 2b).

The other prominent length scale of the network is the mesh size (ζ) (Figure 3). With increasing nanotube loading, ζ decreases and exhibits a power law ($\zeta \sim p^{-\alpha}$) dependence with α values between 0.3 (± 0.03) and 0.4 (± 0.05) for the three systems. These values of α are significantly weaker than that predicted from fractal arguments[10] ($\alpha = 1/(3 - d_f)$) or from the random contact model for uncorrelated rods ($\alpha = 1$).[11] On the other hand, they are somewhat similar to those expected for diffusion-limited formation of clusters in semidilute concentration regime.[12]

It is anticipated that the network elastic strength is proportional to the number of stress-bearing interparticle junctions. Thus, the values of δ observed for the three nanocomposite series (3.8 ± 0.3, 2.5 ± 0.2, and 2.5 ± 0.4 for PEO, BA, and BF systems, respectively) are not easily reconciled in the context of the composition invariant floc size and the weak crowding of the mesh within a floc. On the other hand, the Guinier prefactor of the highest structural level (G_1) is loosely connected with the number of flocs
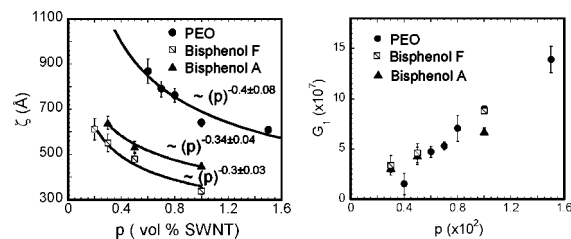
Figure 3. Concentration dependence of the network mesh size (ζ) and the Guinier prefactor of the highest structural level (G_1) in different matrices. The scaling of ζ is consistent with diffusion-limited cluster formation, while the dependence of G_1 suggests that the number of flocs grows linearly with the concentration of nanotubes. The error bars shown here and in the rest of the paper correspond to ±1 standard deviation, obtained from the fitting of the scattering data to the model.

present in the system and shows a near linear dependence with nanotube concentration ($\sim p^{1.1 \pm 0.1}$) and suggests that the interactions between flocs (directly or mediated) do control the concentration dependence of the elastic strength of the network.

Further, evidence for the notion that the interactions between flocs mediated by the polymer dominate the elastic properties comes from an examination of the absolute magnitude of the network strength and, in particular, examination of the behavior of the specific elastic strength G_{SP} ($=G_{network}/(p - p_c)^\delta$) as a function of p_c. We observe that the G_{SP} scales inversely with p_c ($G_{SP} = 1.54 \times 10^4$, 2.7×10^3, 1.5×10^3 dynes/cm^2 for PEO, BA, and BF with p_c values of 0.09, 0.20, and 0.25 vol %, respectively) and suggests that G_{SP} is a measure of the interactions between the polymer and the clusters of nanotubes: the stronger the interaction between nanotubes and the media, the lower the percolation threshold and the higher specific elastic strength of the network. It would be worthwhile to see if this notion of interfloc interactions controlling the elastic response and the use if the specific elastic strength can be extended to other such dispersions.

Supporting Information Available: Experimental details, model fitting, and supplementary experimental evidence. This material is available free of charge via the Internet at http://pubs.acs.org.

References
(1) (a) Chatterjee, T.; Krishnamoorti, R. *Phys. Rev. E* **2007**, *75*, 050403. (b) Chatterjee, T.; Mitchell, C. A.; Hadjiev, V. G.; Krishnamoorti, R. *Adv. Mater.* **2007**, *19*, 3850.
(2) (a) Hobbie, E. K.; Fry, D. J. *Phys. Rev. Lett.* **2006**, *97*, 036101. (b) Rueb, C. J.; Zukoski, C. F. *J. Rheol.* **1997**, *41*, 197. (c) Trappe, V.; Weitz, D. A. *Phys. Rev. Lett.* **2000**, *85*, 449.
(3) Prasad, V.; Trappe, V.; Dinsmore, A. D.; Segre, P. N.; Cipelletti, L.; Weitz, D. A. *Faraday Discuss.* **2003**, *123*, 1.
(4) Larson, R. G. *The Structure and Rheology of Complex Fluids*, 1st ed.; Oxford University Press: New York, 1999.
(5) Chatterjee, T.; Yurekli, K.; Hadjiev, V. G.; Krishnamoorti, R. *Adv. Funct. Mater.* **2005**, *15* (11), 1832.
(6) (a) Barker, J. G.; Glinka, C. J.; Moyer, J. J.; Kim, M. H.; Drews, A. R.; Agamalian, M. *J. Appl. Crystallogr.* **2005**, *38*, 1004. (b) Glinka, C. J.; Barker, J. G.; Hammouda, B.; Krueger, S.; Moyer, J. J.; Orts, W. J. *J. Appl. Crystallogr.* **1998**, *31*, 430.
(7) (a) Brown, J. M.; Anderson, D. P.; Justice, R. S.; Lafdi, K.; Belfor, M.; Strong, K. L.; Schaefer, D. W. *Polymer* **2005**, *46*, 10854. (b) Schaefer, D. W.; Zhao, J.; Brown, J. M.; Anderson, D. P.; Tomlin, D. W. *Chem. Phy. Lett.* **2003**, *375*, 369.
(8) Beaucage, G. *J. Appl. Crystallogr.* **1996**, *29*, 134.
(9) Kline, S. R. *J. Appl. Crystallogr.* **2006**, *39*, 895.
(10) Shih, W. H.; Shih, W. Y.; Kim, S. I.; Liu, J.; Aksay, I. A. *Phys. Rev. A* **1990**, *42*, 4772.
(11) Philipse, A. P. *Langmuir* **1996**, *12*, 5971.
(12) Schmidt, C. F.; Barmann, M.; Isenberg, G.; Sackmann, E. *Macromolecules* **1989**, *22*, 3638.

JA801480H